J Math Chem (2009) 46:303–321
DOI 10.1007/s10910-008-9463-7

ORIGINAL PAPER

Analysis of a chemostat model with variable yield coefficient: Tessier kinetics

M. I. Nelson · H. S. Sidhu

Received: 11 August 2008 / Accepted: 2 September 2008 / Published online: 26 September 2008

Abstract We investigate a chemostat model in which the growth rate is given by a Tessier expression with a variable yield coefficient. We combine analytical results with path-following methods. The washout conditions are found. When washout does not occur we establish the conditions under which the reactor performance and reactor productivity are maximised. We also determine the parameter region in which oscillations may be generated in the reactor. We briefly discuss the implications of our results for comparing the performance of a single bioreactor against a cascade of two bioreactors.

Keywords Bioreactors · Bifurcation · Continuous culture · Nonlinear dynamics · Reaction engineering · Stability · Variable yield

Nomenclature

F Flowrate ($1\,h^{-1}$)
K_s Tessier constant ($g\,l^{-1}$)
P Reactor productivity $P = F \cdot X_s$ ($g\,h^{-1}$)
P^* Dimensionless reactor productivity $P^* = \frac{P}{\alpha \mu_m K_s V}$ (–)
S Substrate concentration ($g\,l^{-1}$)

M. I. Nelson (✉)
School of Mathematics and Applied Statistics, The University of Wollongong, Wollongong, NSW 2522, Australia
e-mail: nelsonm@member.ams.org; mnelson@uow.edu.au

H. S. Sidhu
School of Physical, Environmental and Mathematical Science, UNSW at ADFA, Canberra, ACT 2600, Australia
e-mail: h.sidhu@adfa.edu.au

S^*	Dimensionless substrate concentration $S_i^* = \frac{S_i}{K_s}$ (–)
S_0	Substrate concentration in the feed ($\mathrm{g\,l^{-1}}$)
S_0^*	Dimensionless substrate concentration in the feed $S_0^* = \frac{S_0}{K_s}$ (–)
V	Reactor volume (l)
X	Cell mass concentration ($\mathrm{g\,l^{-1}}$)
X_s	Steady-state cell mass concentration ($\mathrm{g\,l^{-1}}$)
X^*	Dimensionless cell mass concentration $X_i^* = \frac{X_i}{\alpha K_s}$ (–)
$X*_{\max}$	The maximum (physically meaningful) value of the cell mass concentration on the no-washout solution branch (–)
X_0	Cell mass concentration in the feed ($\mathrm{g\,l^{-1}}$)
X_0^*	Dimensionless cell mass concentration in the feed $X_0^* = \frac{X_0}{\alpha K_s}$ (–)
X_2^*	Cell mass concentration in the second reactor of a cascade (–)
$Y(S)$	Cell mass yield coefficient (–)
t	Time (h)
t^*	Dimensionless time $t^* = \mu_m t$ (–)
α	Constant in yield coefficient (–)
β	Constant in yield coefficient ($\mathrm{l\,g^{-1}}$)
β^*	Dimensionless yield coefficient $\beta^* = \frac{\beta K_s}{\alpha}$ (–)
$\mu(S)$	Specific growth rate ($\mathrm{h^{-1}}$)
μ_m	Maximum specific growth rate ($\mathrm{h^{-1}}$)
τ	Residence time $\tau_i = \frac{V_i}{F}$ (h)
τ^*	Dimensionless residence time $\tau_i^* = \mu_m \cdot \frac{V_i}{F}$ (–)
$\tau^*_{\max}$	The value of τ^*, should it exist, at which the dimensionless cell mass concentration obtains its maximum value ($X^*_{\max}$) (–)
τ_i^*	The dimensionless residence time in the ith bioreactor in a bioreactor cascade.
τ_t^*	The total dimensionless residence time in a cascade of two bioreactors.
	Parameter values $K_s = 1.75\,\mathrm{g\,l^{-1}}$, $\alpha = 0.01$, $\beta = 0.031\,\mathrm{g^{-1}}$, $\mu_m = 0.3\mathrm{h^{-1}}$. These give $\beta^* = 5.25$

1 Introduction

There are several well-known kinetic models for the specific growth-rate of cell mass in bioreactors, including those of Tessier [1], Monod [2], Moser [3], Contois [4] and Andrews [5]. In this paper we investigate the behaviour of a continuously stirred bioreactor in which the specific growth-rate is given by a Tessier expression with a variable yield coefficient. We determine the conditions for washout to occur, the conditions under which the cell mass concentration inside the reactor is maximised, the conditions under which the reactor productivity (the product of cell mass concentration with flow-rate through the reactor) is maximised and the conditions for self-sustained oscillations to be generated within the chemostat.

The conditions under which a *steady* input of reactants can generate self-sustained oscillations as an output from a single reactor are of interest because of the possibility

of using this output to force a second reactor. This has the potential of achieving the advantages relating to the periodic forcing of a chemical reactor without the additional costs associated implementing external periodic forcing [6–10]. Understanding the behaviour of a *single* reactor is a pre-requisite to understanding the correct design of a two-reactor cascade [11]. Firstly, the conditions under which the second reactor is forced by the output from the first reactor are purely determined by the dynamics of the latter. Secondly, the maximum output from the single reactor system provides a benchmark for comparing the performance of a two-reactor cascade. Thus in this paper we present an analysis of the Tessier model in a single bioreactor. Although the focus of this paper is a single bioreactor, we briefly discuss the implications of our results for the analysis of a two-reactor cascade in Sect. 4.

1.1 Review of related work

In Sect. 1.1.1 we note some biochemical systems which have been shown to obey Tessier kinetics. In Sect. 1.1.2 we outline some of the investigations that have been carried out into systems with a variable yield. (We exclude from this section investigations based upon Tessier kinetics; they are described in the next section.) In Sect. 1.1.3 we describe mathematical investigations into systems based upon Tessier kinetics, including results for systems with constant and non-constant yields.

1.1.1 Experimental systems described by Tessier kinetics

It is not possible to provide a comprehensive overview of biological systems that have been found to obey Tessier kinetics. We limit ourselves to outlining a few such systems.

Sönmezişik et al. [12] showed that a double substrate model with both Tessier and Moser growth kinetics represented the experimental data for the growth of *Suffolobus solfataricus*, a thermophilic sulfur-removing archeabacterium, reasonably well.

McHenry and Werker [13] showed that the Tessier growth model was the most suitable to characterize bioactivity in treatment wetlands.

Yurt et al. [14] showed that a model combining Monod growth kinetics for pyruvate and Tessier growth kinetics for oxygen showed the best correlation with experimental data for *Leptothrix discophora* SP-6 (a manganese—and iron-oxidizing sheathed bacteria that thrive in both iron—and manganese-rich environments).

Beyenal et al. [15] showed that a Tessier growth expression based upon a dual-substrate model, oxygen and glucose, had good agreement with experimental chemostat data describing the growth kinetics of *Pseudomonas aeruginosa* (a microbial that is often used in biofilm studies and for modelling biofilm accumulation).

1.1.2 Models with a variable yield coefficient

Crooke et al. [16] showed that simple chemostat models of the form given by Eqs. 1 and 2 cannot have periodic solutions for *any* choice of the specific growth function $\mu(S)$ if the yield is constant. However as biological system have an ubiquity for periodicity

this result motivated an interest in deriving simple extensions of the system (1) and (2) which do exhibit periodicity. Numerical solutions presented in [16] showed that limit cycles can be observed under certain circumstances if the yield coefficient is a function of the substrate concentration. (The use of a variable yield coefficient had been suggested earlier by Essajee and Tanner [17].) These findings motivated the initial investigations into systems with a variable yield carried out by Crooke and Tanner [18] and Agrawal et al. [19].

Crooke and Tanner [18] showed that when Monod growth rate kinetics are assumed

$$\mu(S) = \frac{\mu_m}{K + S},$$

Hopf bifurcations can occur when the yield coefficient, Eq. 4, increases linearly with substrate concentration. In the same year Agrawal et al. [19] established conditions for Hopf bifurcations to occur in a model with a general growth rate function, $\mu(S)$, and a general yield function, $Y(S)$. They showed that a Hopf bifurcation will occur provided that the yield coefficient increases 'sufficiently fast' as a function of the substrate concentration. (Their result provides another proof of the result established by Crooke et al. [16] that a Hopf bifurcation can not occur for systems with a constant yield.) Since these pioneering studies, subsequent research has often split into those investigations using specific growth rate and yield functions and those using general growth rate and yield functions.

Agrawal et al. [19] considered two expressions for the specific growth rate: Monod kinetics and a substrate inhibition model. For both models they established parameter regions in which the steady-state diagram contains two Hopf bifurcation points.

Other investigators have considered the two-component system with Monod kinetics and a linear yield [10,11,20,21]. Yang and Su [10] investigated the productivity of a cascade of two reactors. They fixed the total residence time of the cascade and varied the residence time in the first reactor. By choosing appropriate parameters it is possible to ensure that the stable attractor in the first reactor is a limit cycle. These oscillations then force the second reactor. Their primary interest was whether such forcing could increase the productivity of the cascade. They showed that in some circumstances an "enormous improvement" in performance could be obtained, compared to a single reactor of the same residence time. Nelson and Sidhu [11] re-investigated the model considered by Yang and Su [10], arguing that Yang and Su had over-estimated the increase in performance that can be achieved by a cascade because they had not compared "like with like": the performance of the optimal cascade had not been compared against the optimal performance of a single reactor. Balakrishnan and Yang [20] investigated numerically the productivity of a single reactor as a function of the residence time. Nelson and Sidhu [21] re-investigated the behaviour of a single reactor, identifying the residence time which maximised the biomass concentration in the effluent.

Wu and Chang [22] considered the two-component system with Monod kinetics and a variable yield of the form $(A + BS)^{\gamma}$. Their aim was to derive a control scheme which could be used to eliminate self-generated oscillations from the system. Their scheme was shown to be successful in one simulation.

It is natural to consider a general class of two-component model in which the growth rate law, $\mu(S)$ is assumed to be monotonic, subject to $\mu(0) = 0$, and in which the yield coefficient, $Y(S)$, is strictly positive, subject to $Y(0) = 1$ [19,23–27]. Agrawal et al. [19] showed that such systems have a unique non-washout solution and established conditions for the non-washout solution to lose stability at a Hopf bifurcation. Huang [23] used the Poincaré-Bendixson theorem to show that when the no-washout solution is unstable there exists at least one limit cycle. This general results was applied to a system governed by Monod kinetics with a linearly increasing yield coefficient. Pilyugin and Waltman [24] investigated the global stability of the steady-state solutions. They establish conditions showing that when the no-washout solution branch loses stability at a sub-critical Hopf bifurcation that there is a range of parameter values over which there are at least two limit cycles. It was shown that a subcritical bifurcation can not occur for a system with Monod kinetics if the yield varies linearly with the substrate concentration but it can if the yield takes the form $Y(S) = 1 + cS^2$. The finding of two limit cycles was extended by Zhu and Huang [27], who found conditions that guarantee that there exist at least three limit cycles. Zhu and Huang [26] constructed an annular region with the property that all limit cycles of the system must be contained within it. Finally, Sun and Chen [25] investigated the dynamics of a system in which the substrate concentration is subject to a periodically impulsive perturbation. They found conditions under which the boundary periodic solution is globally asymptotically stable. As the size of the perturbation is varied the system exhibits a range of complex dynamics.

A number of authors have investigated models in which two species compete for the same substrate [24,28–31]. Of interest in these investigations is whether the two species can co-exist. These papers can be classified into two types, depending upon if one of the species produces a substance that is toxic to the other species or not. We first consider those papers where no toxin is produced [24,28,30]. In [24,28] Monod kinetic are used for both species whilst in [30] general growth rate expressions $\mu(S)$ are used.

Pilyugin and Waltman [24] showed numerically that both species can co-exist periodically when one of them has a constant yield coefficient and the other has a variable yield coefficient ($Y(S) = 1 + 50S^3$). Huang and Zhu [28] studied the system with quadratic yields ($A + BS^2$ and $C + DS^2$). It is assumed that one of the species has a natural death-rate whilst the other does not. The stability of the steady state solutions was discussed. The Hopf bifurcation theorem is applied to the two subsystems that arise when one of the species becomes extinct. When this happens, the model reduces to one covered by the results in [23]. Conditions were proved that guarantees a parameter region over which two limit cycles coexist surround an asymptotically stable steady-state solution. Zhu [32] has shown that for systems with Monod kinetics the assumption of a non-constant yield coefficient is not necessary for periodicity as a Hopf bifurcation can occur when both yield coefficients are constant.

Huang et al. [30] considered a model with general growth rates and general variable yields. They investigated the stability of the steady-state solutions. When one of the species is driven to extinction the model reduces to a special case of the system considered in [23] and results on the existence of a limit cycle follow immediately. They established the condition under which a Hopf bifurcation occurs when one of

the species is driven to extinction. They did not investigate whether the resulting periodic solutions can be continued into a parameter region in which it can support both species, as demonstrated numerically by Pilyugin and Waltman [24].

The system in which one species produces a toxin has been investigated in [29, 31,33]. In [31] Monod growth rates are assumed for both species and the yields are given by $A_1 + B_1 S^m$ and $A_2 + B_2 S^n$. An equation for the concentration of the toxin is not included. Huang and Zhu [31] discussed the stability of steady-state solutions and showed the existence of limit cycles through use of the Hopf bifurcation theorem.

In [29] Monod growth rates are assumed for both species and the yields are quadratic ($A_i + B_i S + C_i S^2$). The system has four components as an equation is included for the concentration of the 'toxin'. (In this approach the 'toxin' is considered to be an inhibitor.) This system has a special structure which enables it to reduced to a three-variable system. The asymptotic behaviour of the three-variable system is analyzed and it is shown that the steady-state solution in which the two species co-exist is always unstable. When one of the species is driven to extinction the model reduces to a special case of the two-dimensional system considered in [23] and results on the existence of a limit cycle follow immediately. The conditions for a three dimensional Hopf bifurcation to occur are derived. (Huang et al. [34] have shown that the assumption of non-constant yields is not required for periodicity. A three-dimensional Hopf bifurcation can occur in this model when the yields are constant.) Zhu et al. [33] have extended the results presented in [29] to the case of general yield functions, subject to the restrictions that $Y_i\,(0) = 0$ and $Y_i' \geq 0$. The theorems in this paper are valid in the limiting case when no toxin is produced and therefore generalize many of the results noted in this section up to this point.

We now consider papers where the underlying kinetic model is given by the Andrews inhibition law [5]

$$\mu(S) = \frac{\mu_m S}{K + S + S^2/K_i}.$$

Suzuki et al. [35] investigated the dynamics when a single species grows on a substrate with a linear yield. They obtained the regions in parameter space in which different dynamic behaviour can be observed. Subsequently Shimizu and Matsubara [36] investigated the effect of P-control and PI-control upon the dynamics of this system. Wu et al. [37] have investigate a double-substrate interactive model in which a microorganism grows in the presence of two limiting substrates. The yield factor for one of the substrates was constant whilst the other could either be constant or a linear function of limiting substrate. A Hopf bifurcation can not occur when both yields are constant.

The investigations detailed in the preceeding discussion assumed that the growth rate law was of the form $\mu\,(S)$, as do the papers discussed in Sect. 1.1.3. Recently Nelson et al. [38,39] have investigated the dynamics of a system with Contois growth kinetics

$$\mu(S, X) = \frac{\mu_m S}{KX + S},$$

and a linear yield. These investigations were motivated by experimental studies which have shown that the rate determining step in the cleaning of wastewaters and slurries from a variety of agricultural processes is governed by the Contois expression [40]. In [38] a well-stirred reactor was considered whereas in [39] a well-stirred membrane reactor was considered. A common feature of interest in [38,39] is the considerable decrease in effluent concentration that can be achieved by using a cascade of two reactors rather than a single reactor. In these systems Hopf bifurcations are undesirable because, compared against the effluent concentration at the unstable steady-state solution, they increase the average effluent concentration leaving the reactor.

1.1.3 Tessier kinetics

In [41–43] results have been obtained for the Tessier growth model when a single reactor is subject to *external* periodic forcing.

Liu and Wu [41] showed that the performance of a bioreactor, measured at its optimal steady-state, can not be improved when the flow rate is forced sinusoidally. This holds for Monod, Moser, Tessier and Andrew growth models for both constant and non-constant yield coefficients, $\beta = 0$ and $\beta > 0$ in Eq. 4, respectively.

Liu et al. [42] have shown that it is possible to distinguish between Monod, Moser, Tessier and Contois kinetic models though frequency response analysis when the flow-rate, F in Eqs. 1 and 2, is varied sinusoidally. It is also possible to distinguish between models having constant and non-constant yield coefficients, $\beta = 0$ and $\beta > 0$ in Eq. 4, respectively.

Wu et al. [43] compared the biomass production of a continuous bioreactor with a cyclic feed concentration against that produced under optimal steady-state operation. They considered Monod, Moser, Tessier and Andrew growth models. For Tessier growth, periodic operation can not improve the reactor performance when the yield coefficient is constant, $\beta = 0$ in Eq. 4. They found that for a non-constant yield coefficient ($\beta > 0$) a cyclic feed may improve the performance of a system with Tessier growth. Whether cyclic feeding improves reactor performance when $\beta > 0$ depends upon the value of the substrate concentration in the feed (S_0).

2 Model equations

We investigate a microbial system in which cell mass (X) grows through consumption of a substrate species (S). The specific growth rate, Eq. 3, is given by a Tessier expression with variable yield coefficient, Eq. (4). The objective is to either maximize the cell mass concentration leaving the reactor as a function of the residence time or the reactor productivity ($P = FX$). This model was evidently one of a number of microbial systems investigated by Chen et al. [7], although they only reported numerical results for Monod growth kinetics.

The dimensional and dimensionless forms of our model are stated in Sects. 2.1 and 2.2, respectively.

2.1 Dimensional model

The governing equations of our system are given by

$$V\frac{\mathrm{d}S}{\mathrm{d}t} = F\,(S_0 - S) - V X \frac{\mu(S)}{Y(S)} \tag{1}$$

$$V\frac{\mathrm{d}X}{\mathrm{d}t} = F\,(X_0 - X) + V X \mu(S) \tag{2}$$

Specific growth rate equation

$$\mu(S) = \mu_m \left(1 - \exp\left[-\frac{S}{K_s}\right]\right) \tag{3}$$

Yield Coefficient.

$$Y(S) = \alpha + \beta S, \quad (\alpha, \beta > 0)\,. \tag{4}$$

The terms that appear in Eqs. 1–4 are defined in the nomenclature. Crooke et al. [16] have proved that solutions to the system defined by Eqs. 1 and 2 cannot be periodic in time for *any* choice of the function $\mu\,(S)$ when $\beta = 0$.

2.2 Dimensionless equations

By introducing dimensionless variables for the substrate concentrations ($S^* = S/K_s$), the cell mass concentrations ($X^* = X/\,(\alpha K_s)$) and time ($t^* = \mu_m t$) the system of differential Eqs. 1 and 2 can be written in the dimensionless form

$$\frac{\mathrm{d}S^*}{\mathrm{d}t^*} = \frac{1}{\tau^*}\left(S_0^* - S^*\right) - \frac{X^*\left(1 - \exp\left[-S^*\right]\right)}{1 + \beta^* S^*}, \tag{5}$$

$$\frac{\mathrm{d}X^*}{\mathrm{d}t^*} = \frac{1}{\tau^*}\left(X_0^* - X^*\right) + X^*\left(1 - \exp\left[-S^*\right]\right). \tag{6}$$

The dimensionless model contains four parameters S_0^*, X_0^*, β and τ^*. We consider the case of a sterile feed ($X_0^* = 0$) and take the residence time (τ^*) as the primary bifurcation parameter. The substrate concentration in the feed (S_0^*) and the dimensionless yield coefficient (β^*) are the secondary bifurcation parameters. The value for β^* is determined by the choice of microbial system and is therefore not a 'tunable' parameter.

A feature of our dimensionless scheme is that there is a one-to-one relationship between our dimensionless variables and their dimensional counterparts. Hence we write often, for example, 'the residence time', rather than 'the dimensionless residence time'.

2.3 Numerics

The path-following software Auto 97 [44] was used to obtain the steady-state diagrams. In these the standard representation is used; solid lines are stable steady states; dotted lines are unstable steady states; squares are Hopf bifurcation points; open circles are unstable periodic orbits and filled-in circles are stable periodic solutions. We investigate the reactor performance (X^*) and reactor productivity (X^*/τ^*) as a function of the residence time (τ^*). For a periodic orbit the norm that is used is the integral over the period of the solution.

3 Results

In Sect. 3.1 derive some results for system (5) and (6). In Sect. 3.2 we discuss some numerical results for this system.

3.1 Analytical results: steady-state solutions and their stability

In Sect. 3.1.1 we give the steady-state solutions for system (5) and (6). We note when the no-washout solution branch is physically meaningful and investigate how the maximum value of the cellmass in the effluent stream depends upon system parameters. In Sect. 3.1.2 we investigate the linear stability of the steady-state solutions. In Sect. 3.1.3 we investigate the necessary conditions for a Hopf bifurcation to occur along the no-washout branch. Finally, in Sect. 3.1.5 we determine when the reactor productivity is maximised.

3.1.1 Steady-state solutions

The model (5) and (6) has two steady-state solutions. These represent washout and no-washout in the reactor and are given by
Washout

$$\left(S^*, X^*\right) = \left(S_0^*, 0\right), \tag{7}$$

No-washout

$$\left(S^*, X^*\right) = \left(\ln\left(\frac{\tau^*}{\tau^*-1}\right), \left[S_0^* - \ln\left(\frac{\tau^*}{\tau^*-1}\right)\right]\left[1 + \beta^* \ln\left(\frac{\tau^*}{\tau^*-1}\right)\right]\right). \tag{8}$$

The substrate component of (8) is only defined if $\tau^* > 1$. Given that $\tau^* > 1$ the cell mass component of (8) is non-negative only if

$$\tau^* \geq \frac{\exp\left[S_0^*\right]}{\exp\left[S_0^*\right] - 1} = \frac{1}{1 - \exp\left[-S_0^*\right]}.$$

This is therefore the condition for the no-washout solution to be physically meaningful. The corresponding result for the Monod model is stated in Table 1.

Table 1 Comparison of results for the Tessier model with variable yield coefficient and the Monod model with variable yield coefficient [21]

	Monod	Tessier
Condition for no-washout branch	$\tau^* \geq 1 + \frac{1}{S_0^*}$	$\tau^* \geq \frac{1}{1-\exp[-S_0^*]}$
Condition for a global maximum	$\beta^* S_0^* > 1$	$\beta^* S_0^* > 1$
Residence time at the global maximum	$1 + \frac{2\beta^*}{\beta^* S_0^* - 1}$	$\frac{1}{1-\exp\left[-\frac{\left(S_0^*\beta^* - 1\right)}{2\beta^*}\right]}$
$X^*_{\max}$	$\frac{\left(1+\beta^* S_0^*\right)^2}{4\beta^*}$	$\frac{\left(1+\beta^* S_0^*\right)^2}{4\beta^*}$
Condition for the washout state to be stable	$\tau^* < 1 + \frac{1}{S_0^*}$	$\tau^* < \frac{1}{1-\exp[-S_0^*]}$

It is instructive to investigate how the steady-state performance of the reactor, that is to say the value of the cell mass concentration on the non-washout branch of solutions, varies with the residence time. In particular, we want to determine whether there is a residence time at which the cell mass concentration is maximised.

Calculation shows that

$$\frac{\mathrm{d}X^*}{\mathrm{d}\tau^*} = 0 \Longrightarrow \quad \tau^*_{\max} = \frac{1}{1-\exp\left[-\frac{\left(S_0^*\beta^* - 1\right)}{2\beta^*}\right]}. \tag{9}$$

It follows that if $S_0^*\beta^* > 1$ the steady-state diagram of system performance (X^*) against residence time (τ^*) has a local maximum at the point

$$\left(\tau^*, S^*_{\max}, X^*_{\max}\right) = \left(\tau^*_{\max}, \frac{S_0^*\beta^* - 1}{2\beta^*}, \frac{\left[1+\beta^* S_0^*\right]^2}{4\beta^*}\right). \tag{10}$$

The maximum value of the cell mass concentration using Tessier kinetics with a variable yield coefficient is the *same* as the maximum value of the cell mass concentration using Monod kinetics with a variable yield coefficient (see Table 1).

Conversely, if $\beta^* S_0^* < 1$ then $\tau^*_{\max} < 0$ and the corresponding value of X^* is non-physical. In this case the steady-state performance is maximised at an infinite residence time

$$\lim_{\tau^* \to \infty} X^* = S_0^*.$$

3.1.2 Stability analysis of washout solution

From an operational viewpoint washout must be avoided. In this section we investigate the stability of the washout branch. The Jacobian matrix for washout is

$$J = \begin{pmatrix} -\frac{1}{\tau^*} & -\frac{\left(1-\exp[-S_0^*]\right)}{1+\beta^* S_0^*} \\ 0 & -\frac{1}{\tau^*} + \left(1 - \exp\left[-S_0^*\right]\right) \end{pmatrix}.$$

The eigenvalues of this matrix are

$$\lambda_1 = -\frac{1}{\tau^*},$$
$$\lambda_2 = -\frac{1}{\tau^*} + \left(1 - \exp\left[-S_0^*\right]\right).$$

Thus the washout branch is stable provided

$$\tau^* < \frac{1}{1-\exp[-S_0^*]} = \frac{\exp[S_0^*]}{\exp[S_0^*]-1}.$$

This stability criterion was given by Chen et al. [7, Eq. 10].

3.1.3 Stability of the no-washout branch

In this section we analyze the stability of the steady-state given by Eq. 8. Note that this steady-state is only physically meaningful for $\tau^* \geq \frac{1}{1-\exp[-S_0^*]} > 1$. The Jacobian matrix for the no washout state is

$$J = \begin{pmatrix} J_{11} & J_{12} \\ J_{21} & 0 \end{pmatrix} \tag{11}$$

where

$$J_{11} = -\frac{1}{\tau^*} - \left[S_0^* - \ln\left(\frac{\tau^*}{\tau^*-1}\right)\right]\left[\frac{\tau^*-1}{\tau^*} - \frac{\beta^*}{2\tau\left[1+\beta^*\ln\left(\frac{\tau^*}{\tau^*-1}\right)\right]}\right],$$
$$J_{12} = -\frac{1}{\tau^*\left[1+\beta^*\ln\left(\frac{\tau^*}{\tau^*-1}\right)\right]},$$
$$J_{21} = \frac{\tau^*-1}{\tau^*}\cdot\left[S_0^* - \ln\left(\frac{\tau^*}{\tau^*-1}\right)\right]\left[1+\beta^*\ln\left(\frac{\tau^*}{\tau^*-1}\right)\right].$$

The Jacobian matrix (11) has a zero eigenvalue when $J_{11}J_{22} - J_{12}J_{21} = 0$. This requires τ^* to take the value 1 or $\frac{1}{1-\exp[-S_0^*]}$. Only the latter condition is meaningful.

The condition for a double-zero eigenvalue are $J_{11}J_{22} - J_{12}J_{21} = 0$ and $J_{11} + J_{22} = 0$ [45]. By inspection these conditions can not be satisfied with $S_0^* > 0$. Thus a double-zero eigenvalue can not occur.

We know that when $\tau^* \geq \frac{1}{1-\exp[-S_0^*]}$ there is a value of the residence time that maximizes the reactor performance. The values for the substrate and cell mass concentrations at this point are given by Eq. 10. From the Jacobian matrix (11) this point is stable if

$$\mathrm{tr}J = J_{11} + J_{22} < 0,$$
$$\det J = J_{11}J_{22} - J_{12}J_{21} > 0.$$

After some algebraic manipulation we obtain

$$J_{11} + J_{22} = -\frac{\left(1+\beta^* S_0^*\right)}{2\beta^*} \cdot \exp\left[\frac{1 - S_0^* \beta^*}{2\beta^*}\right] < 0,$$
$$J_{11}J_{22} - J_{12}J_{21} = \frac{1+\beta^* S_0^*}{2\beta^*}\left(1 - \exp\left[\frac{1-\beta^* S_0^*}{2\beta^*}\right]\right)\exp\left[\frac{1-\beta^* S_0^*}{2\beta^*}\right].$$

As $X^*_{\max}$ only exists if $\beta^* S_0^* - 1 > 0$ we conclude that $J_{11}J_{22} - J_{12}J_{21} > 0$ and consequently the point $(S^*_{\max}, X^*_{\max})$ is *always* stable and therefore has practical importance.

3.1.4 Hopf bifurcation on the no-washout state

The condition for a Hopf bifurcation is $J_{11} + J_{22} = 0$ with $J_{11}J_{22} - J_{12}J_{21} > 0$ [45]. The latter is always satisfied. The values of the residence time at which Hopf bifurcations satisfy the equation

$$\mathcal{H} = -S_0^*\left(\tau^* - 1 - \beta^*\right) - 1 - \left[\left(\tau^* - 1\right)\beta^* S_0^* - \left(\tau^* - 1 - 2\beta^*\right)\right]\ln\left(\frac{\tau^*}{\tau^* - 1}\right) + \left(\tau^* - 1\right)\beta^* \ln^2\left(\frac{\tau^*}{\tau^* - 1}\right) \tag{12}$$

subject to the constraint $\tau^* \geq \frac{1}{1-\exp[-S_0^*]}$. (It is possible to show that this equation has no solutions when $\beta^* = 0$.) With $\beta^* = 5.25$ and $S_0^* = 20$, the parameter values used for Fig. 1a, Eq. 12 has zeroes at $\tau^* = 1.00005$ and $\tau^* = 2.209$. These are the values of the residence time corresponding to Hopf bifurcation points.

A degenerate Hopf bifurcation at which two Hopf points annihilate each other in an unfolding diagram (a $H2_1$ degeneracy) occurs when the following conditions are satisfied [45].

$$\begin{aligned} \mathcal{H} &= 0, \\ \frac{d\mathcal{H}}{d\tau^*} &= 0. \end{aligned} \tag{13}$$

When applied to Eq. 12 these conditions give the following system of equations

$$S_0^* = \frac{-(\tau^*-1-2\beta^*)+(\tau^*-1)(\tau^*-2\beta^*)\ln\left(\frac{\tau^*}{\tau^*-1}\right)+\tau^*(\tau^*-1)\beta^*\ln^2\left(\frac{\tau^*}{\tau^*-1}\right)}{(\tau^*-1)\left[\tau^*-\beta^*+\tau^*\beta^*\ln\left(\frac{\tau^*}{\tau^*-1}\right)\right]}, \tag{14}$$

$$\left(\tau^* - 1\right)\left(1 + 2\beta^*\right) - 2\beta^{*^2} = -\left(\tau^* - 1\right)\beta^{*^2}\ln^2\left(\frac{\tau^*}{\tau^* - 1}\right) - 2\left(\tau^* - 1\right)\left(1 + \beta^*\right)\beta^* \ln\left(\frac{\tau^*}{\tau^* - 1}\right). \tag{15}$$

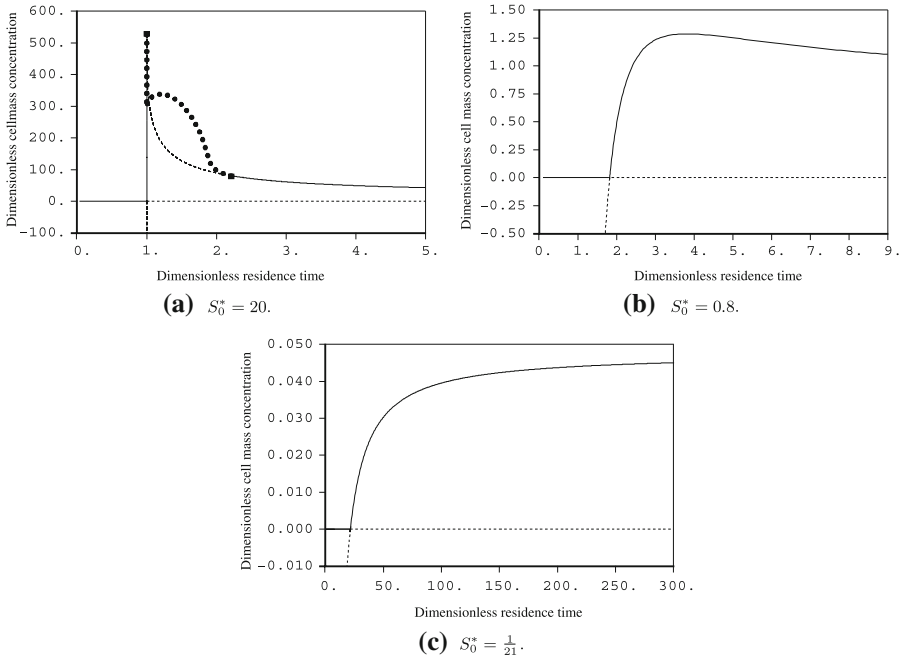

(a) $S_0^* = 20.$ **(b)** $S_0^* = 0.8.$

(c) $S_0^* = \frac{1}{21}.$

Fig. 1 Steady-diagrams showing the variation of reactor performance (X^*) with residence time (τ^*). Parameter value: yield constant, $\beta^* = 5.25$

When $\beta^* = 5.25$ the solution of these equations is

$$\left(S_0^*, \tau^*\right) = (4.67, 1.408)\,. \tag{16}$$

From this analysis we conclude the natural oscillations are impossible for one of the cases: $S_0^* < 4.67$ or $S_0^* > 4.67$. Comparing Fig. 1a and b we see that natural oscillations do not occur in this system for $S_0^* < 4.67$.

3.1.5 Maximum productivity

The dimensionless reactor productivity is defined by

$$P^* = \frac{X^*}{\tau^*}. \tag{17}$$

The value of the residence time at which the productivity is maximised is determined by

$$\frac{\mathrm{d}P^*}{\mathrm{d}\tau} = 0 \Longrightarrow$$

$$S_0^* \left(\tau^* + \beta^* - 1\right) + 1 = \left(\tau^* - 1\right) \beta^* \ln^2 \left(\frac{\tau^*}{\tau^* - 1}\right) + \left[2\beta^* - \left(\tau^* - 1\right)\left(\beta^* S_0^* - 1\right)\right] \ln \left(\frac{\tau^*}{\tau^* - 1}\right). \quad (18)$$

For example, when $\beta^* = 5.25$ and $S_0^* = 20$ the productivity is maximised when $\tau^* = 1.000050$ and is $P_{\max}^* = 535.021$.

3.2 Numerical results

Figure 1 shows three steady-state diagrams. The first steady-state diagram contains two Hopf points. In the second and third steady-state diagrams there are no Hopf points as the inflowing substrate concentration is below that corresponding to the $H2_1$ degeneracy. In (a and b) $S_0^* \beta^* > 1$ so that the steady-state value of the reactor-performance (X^*) is maximised at a finite value of the residence time. For the given value of the yield coefficient the maximum cell mass is given by: $X_{\max}^* = 535$, Fig. 1a, and $X_{\max}^* = 1.288$, Fig. 1b. In Fig. 1c $S_0^* \beta^* < 1$, so that the system performance increases monotonically with the residence system.

The two Hopf bifurcation points in Fig. 1a are unfolded with the substrate concentration in the feed in Fig. 2. This shows that as the substrate concentration is decreased the two Hopf points annihilate each other at a $H2_1$ degeneracy. The parameter values at the degeneracy are given in Eq. 16. For values of the feed substrate concentration greater than the value at the $H2_1$ degeneracy the Hopf locus defines the values of the residence time at which a Hopf bifurcation occurs and consequently defines the parameter values over which periodic solutions occur. The figure also shows the value

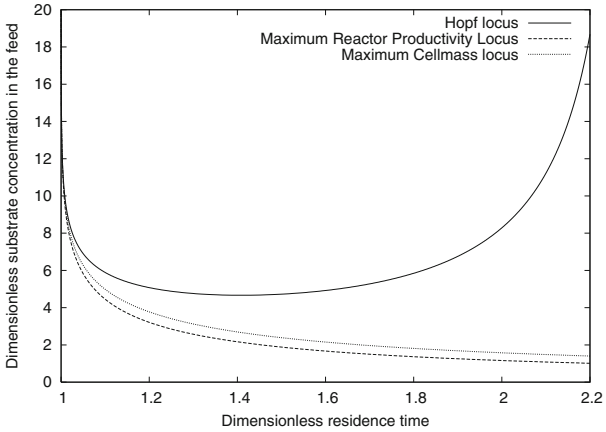

Fig. 2 Unfolding diagram showing the Hopf bifurcation locus, the residence time at which the steady-state cell mass concentration (X^*) is maximised and the residence time at which the reactor productivity ($P^* = X^*/\tau^*$) is maximised. Parameter value: yield constant, $\beta^* = 5.25$

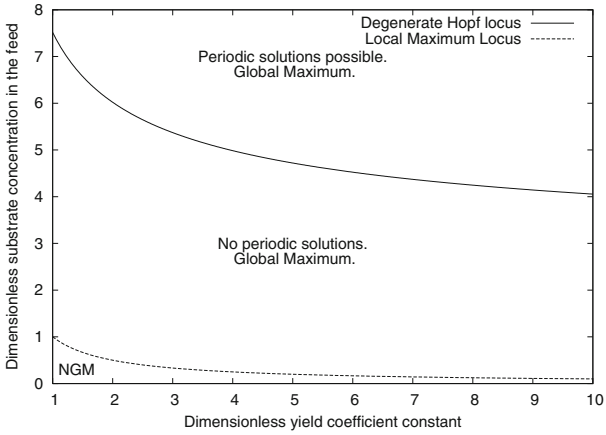

Fig. 3 Bifurcation diagram showing the $H2_1$ locus and the transition from a steady-state diagram having a local maximum to not having a global maximum (NGM). This figure defines the parameter regions in which the steady-state diagrams shown in Fig. 1 are found

of the residence time at which the reactor productivity and the cell mass concentration are maximised as a function of the substrate concentration in the feed. For a fixed value of the feed substrate concentration we see that the reactor productivity is maximised at a lower value of the residence time than the cell mass concentration.

Figure 3 summarizes the information provided in Sect. 3.1.1, on the existence of a global maximum in the cell mass concentration at a finite value of the residence time, and Sect. 3.1.4, on the $H2_1$ degeneracy. The reactor performance has a local maximum at a finite value of the residence time if $S_0^*\beta^* > 1$. However, if $S_0^*\beta^* < 1$ then the reactor performance is optimized at infinite residence time. For a fixed value of the yield coefficient the steady-state diagram has *no* Hopf points if the value of the inflowing substrate concentration is *below* the $H2_1$ locus and *two* Hopf points if it is above. Thus this figure shows the parameter values in which of the three steady-state diagrams shown in Fig. 1 are to be found.

4 Discussion

In this section we briefly discuss some issues relating to the analysis of a cascade of two bioreactors. We consider a system in which the total residence time, the yield coefficient and the substrate concentration in the feed are fixed to the values stated in the caption of Fig. 4. This figure shows how the cell mass concentration leaving the cascade (X_2^*) depends upon the residence time in the first reactor (τ_1^*). Note that the residence time in the second reactor is defined by $\tau_2^* = 7.5 - \tau_1^*$.

The limits $\tau_1^* = 0$ and $\tau_1^* = 7.5$ represent the degenerate case in which the 'cascade' consists of a single reactor of residence time $\tau^* = 7.5$. The performance of a single reactor with this design parameter is obtained from Eq. 8 as $X^* = 34.8$. The performance of the cascade varies considerably as the reactor-design is varied through the choice of the residence time in the first reactor. The optimal performance of the cas-

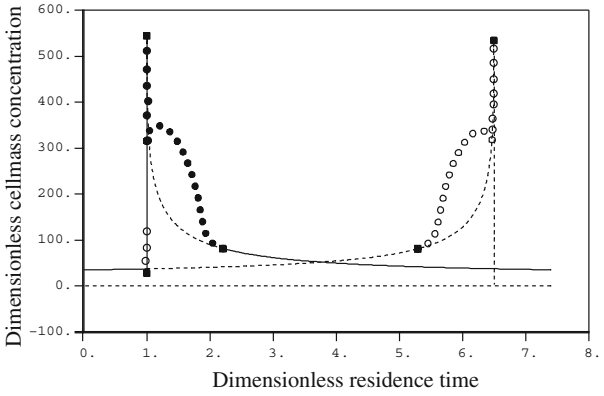

Fig. 4 Dependence of dimensionless cell mass concentration in the second reactor upon the dimensionless residence time in the first reactor for a two-reactor cascade. Parameter values: feed concentration $S_0^* = 20$; total residence time, $\tau_t^* = 7.5$; yield constant, $\beta^* = 5.25$

cade shown in Fig. 4 occurs when $\tau_1^* = 1.00005$ and is given by $X_2^* = 545.145$. This is an increase of 1,467% when compared to a single reactor operating with $\tau^* = 7.5$. Similar results have led other researchers to suggest that a two-bioreactor cascade can lead to an enormous improvement in performance compared to a single bioreactor of the same total residence time [6, 10].

However this is not the best basis to compare a cascade and a single reactor [11]. From Eqs. 9 and 10 we find that the cell mass concentration leaving a single bioreactor is maximised when $\tau^* = 1.00005$ and is given by $X_{\max}^* = 535$. The best performance of the cascade is not so spectacular when compared to that of an optimally designed single reactor: an increase of only 1.9%. Furthermore, for these operating conditions the productivity of the optimal single reactor (534.97) is considerable greater than that of the optimized cascade (72.7).

Thus we deduce that prior to maximizing the performance of a two-reactor cascade, we must first consider the performance of a single reactor. In particular, performance of the two configurations should not be compared for the *same* operating conditions (such as the same total residence time). Instead the *best* possible performance for each reactor configuration should be compared.

Finally, Chen et al. [7] have stated that the the optimal steady-state performance of a single bioreactor with Tessier kinetics "cannot be further improved by the reactor splitting". We have shown in this section that this is certainly *not* the case, although the increase may be marginal.

5 Conclusion

We have analyzed microbial growth in a flow reactor using a Tessier growth model with a variable yield coefficient. Where possible we have compared results from this scheme against those corresponding to Monod kinetics with a variable yield coefficient.

For a given value of the yield coefficient (β^*) we have shown that natural oscillations can only occur if the substrate concentration in the feed (S_0^*) is sufficiently high. This is of interest when a reactor cascade is being used with the aim of using natural oscillations generated in the first reactor to force the subsequent reactors.

We have shown that if $\beta^* S_0^* > 1$ then there is a value of the residence time, $\tau_{\max}^*$, given by Eq. 9, at which the steady-state performance of the reactor is maximised, $X_{\max}^*$, given by Eq. 10. If $\beta^* S_0^* < 1$ then the steady-state performance of the reactor is maximised at an infinite residence time, with $X_{\max}^* = S_0^*$.

We also considered a cascade of two bioreactors in which the residence time in the two reactors are varied whilst keeping the total residence time fixed. We suggest that the maximal performance of the cascade, whether measured by the cell mass concentration leaving the reactor or the reactor productivity, should be compared against the corresponding optimal one-reactor system to evaluate the relative increase in performance from using two reactors. The results of this paper provide a benchmark for such a comparison.

Acknowledgements This work was supported by a grant from the Australian Research Council (DP0559177) and from the Special Research Grant scheme from UNSW at ADFA.

References

1. G. Tessier, Les lois quantitatives de la croissance. Annales de Physiologie et de Physiochimie Biologique **12**, 527–573 (1936)
2. J. Monod, The growth of bacterial culture. Annu. Rev. Microbiol. **3**, 371–394 (1949)
3. H. Moser, *The dynamics of bacterial populations maintained in the chemostat. Publication 614* (Carnegie Institution of Washington, Washington, 1958)
4. D.E. Contois, Kinetics of bacterial growth: relationship between population density and specific growth rate of continuous cultures. J. Gen. Microbiol. **21**, 40–50 (1959)
5. J.F. Andrews, A mathematical model for the continuous culture of microorganisms utilizing inhibitory substrate. Biotechnol. Bioeng. **10**(6), 707–724 (1968)
6. A. Balakrishnan, R.Y.K. Yang, Improvement of chemostat performance via nonlinear oscillations. Part 2. Extension to other systems. ACH—Models Chem. **135**(1–2), 1–18 (1998)
7. C.-C. Chen, C. Hwang, R.Y.K. Yang, Performance enhancement and optimization of chemostat cascades. Chem. Eng. Sci. **50**(3), 485–494 (1995)
8. S. Jianqiang, A.K. Ray, Performance improvement of activated sludge wastewater treatment by nonlinear natural oscillations. Chem. Eng. Technol. **23**(12), 1115–1122 (2000)
9. A.J. Ray, Performance improvement of a chemical reactor by non-linear natural oscillations. Chem. Eng. J. **59**, 169–175 (1995)
10. R.Y.K. Yang, J. Su, Improvement of chemostat performance via nonlinear oscillations. Part 1: operation strategy. Bioprocess Eng. **9**, 97–102 (1993)
11. M.I. Nelson, H.S. Sidhu, Evaluating the performance of a cascade of two bioreactors. Chem. Eng. Sci. **61**(10), 3159–3166 (2006). doi:10.1016/j.ces.2005.12.007
12. M. Sömezişik, D. Tanyolaç, S. Şeker, A. Tanyolaç, The double-substrate growth kinetics of *Sulfolobus solfataricus* a thermophilic sulfur-removing archeabacterium. Biochem. Eng. J. **1**, 243–248 (1998)
13. J. McHenry, A.G. Werker, Characterization of bioactivity in treatment wetlands utilising an enzymatic assay, in *CSCE/EWRI of ASCE Environmental Engineering Conference*, (2002) pp. 1–14
14. N. Yurt, J. Sears, Z. Lewandowski, Multiple substrate growth kinetics of *Leptothrix disophora* SP-6. Biotechnol. Prog. **18**, 994–1002 (2002)
15. H. Beyenal, S.N. Chen, Z. Lewandowski, The double substrate growth kinetics of *Pseudomonas aeruginosa*. Enzyme Microb. Technol. **32**, 92–98 (2003)

16. P.S. Crooke, C.-J. Wei, R.D. Tanner, The effect of the specific growth rate and yield expressions on the existence of oscillatory behaviour of a continuous fermentation model. Chem. Eng. Commun. **6**(6), 333–347 (1980)
17. C.K. Essajee, R.D. Tanner, The effect of extracellular variables on the stability of the continuous baker's yeast-ethanol fermentation process. Process Biochem. **14**, 16–25 (1979)
18. P.S. Crooke, R.D. Tanner, Hopf bifurcations for a variable yield continuous fermentation model. Int. J. Eng. Sci. **20**(3), 439–443 (1982)
19. P. Agrawal, C. Lee, H.C. Lim, D. Ramkrishna, Theoretical investigations of dynamic behaviour of isothermal continuous stirred tank biological reactors. Chem. Eng. Sci. **37**, 453–462 (1982)
20. A. Balakrishnan, R.Y.K. Yang, Self-forcing of a chemostat with self-sustained oscillations for product enhancement. Chem. Eng. Commun. **189**(11), 1569–1585 (2002)
21. M.I. Nelson, H.S. Sidhu, Analysis of a chemostat model with variable yield coefficient. J. Math. Chem. **38**(4), 605–615 (2005)
22. W. Wu, H.-Y. Chang, Output regulation of self-oscillating biosystems: model-based proportional-integral/proportional-integral-derivative (pi/pid) control approaches. Ind. Eng. Chem. Res. **46**(12), 4282–4288 (2007)
23. X.-C. Huang, Limit cycles in a continuous fermentation model. J. Math. Chem. **5**, 287–296 (1990)
24. S.S. Pilyugin, P. Waltman, Multiple limit cycles in the chemostat with variable yield. Math. Biosci. **182**, 151–166 (2003)
25. S. Sun, L. Chen, Complex dynamics of a chemostat with variable yield and periodically impulsive perturbation on the substrate. J. Math. Chem. **43**(1), 338–349 (2008)
26. L. Zhu, X. Huang, Relative positions of limit cycles in the continuous culture vessel with variable yield. J. Math. Chem. **38**(2), 119–128 (2005)
27. L. Zhu, X. Huang, Multiple limit cycles in a continuous culture vessel with variable yield. Nonlinear Anal. **64**, 887–894 (2006)
28. X. Huang, L. Zhu, A three-dimensional chemostat with quadratic yields. J. Math. Chem. **38**(3), 399–412 (2005)
29. X. Huang, Y. Wang, L. Zhu, Competition in the bioreactor with general quadratic yields when one competitor produces a toxin. J. Math. Chem. **39**(2), 281–294 (2006)
30. X. Huang, L. Zhu, E.H.C. Chang, Limit cycles in a chemostat with general variable yields and growth rates. Nonlinear Anal.: Real World Appl. **8**, 165–173 (2007)
31. X. Huang, L. Zhu, A note on competition in the bioreactor with toxin. J. Math. Chem. **42**(3), 645–659 (2007)
32. L. Zhu, Limit cycles in chemostat with constant yields. Math. Comput. Model. **45**, 927–932 (2007)
33. L. Zhu, X. Huang, H. Su, Bifurcation for a functional yield chemostat when one competitor produces a toxin. J. Math. Anal. Appl. **329**, 891–903 (2007)
34. X. Huang, L. Zhu, E.H.C. Chang, The 3-D Hopf bifurcation in bio-reactor when one competitor produces a toxin. Nonlinear Anal.: Real World Appl. **7**, 1167–1177 (2006)
35. S. Suzuki, K. Shimizu, M. Matsubara, On the parameter-space classification of the dynamic behaviour of a continuous microbial flow reactor. Chem. Eng. Commun. **33**, 325–335 (1985)
36. K. Shimizu, M. Matsubara, Conditions for the phase-plane analysis of feedback control of chemostat. Biotechnol. Bioeng. **27**(4), 519–524 (1985)
37. S.-C. Wu, S.-H. Shih, H.-S. Liu, Dynamic behaviour of double-substrate interactive model. J. Chin. Inst. Chem. Eng. **38**, 107–115 (2007)
38. M.I. Nelson, H.S. Sidhu, Reducing the emission of pollutants in food processing wastewaters. Chem. Eng. Process. **46**(5), 429–436 (2007). doi:10.1016/j.cep.2006.04.012
39. M.I. Nelson, X.D. Chen, H.S. Sidhu, Reducing the emission of pollutants in industrial wastewater through the use of membrane reactors, in *Aspects of Mathematical Modelling*, ed. by R.J. Hosking, E. Venturino (Birkhäuser, Basel, 2008), pp. 95–107
40. M.I. Nelson, E. Balakrishnan, H.S. Sidhu, X.D. Chen, A fundamental analysis of continuous flow bioreactor models and membrane reactor models to process industrial wastewaters. Chem. Eng. J. **140**(1–3), 521–528 (2008)
41. H.-S. Liu, S.-C. Wu, Periodical operation of continuous bioreactor. J. Chin. Inst. Chem. Eng. **26**(5), 233–243 (1995)
42. H.-S. Liu, S.-C. Wu, S.-C. Lin, Theoretical analysis of frequency response in continuous bioreactor. Chem. Eng. Commun. **164**, 13–34 (1998)

43. S.-C. Wu, C.-C. Lin, H.-S. Liu, Theoretical analysis of a continuous bioreactor subject to cyclic feed concentration. J. Chin. Inst. Chem. Eng. **30**(2), 151–160 (1999)
44. E.J. Doedel, T.F. Fairgrieve, B. Sandstede, A.R. Champneys, Y.A. Kuznetsov, X. Wang, *AUTO 97: continuation and bifurcation software for Ordinary Differential Equations (with HomCont)* (1998), ftp://ftp.cs.concordia.ca/pub/doedel/auto
45. B.F. Gray, M.J. Roberts, A method for the complete qualitative analysis of two coupled ordinary differential equations dependent on three parameters. Proc. Roy. Soc. A, **416**, 361–389 (1988)